Available online at www.sciencedirect.com
SCIENCE DIRECT®
Surface and Coatings Technology 183 (2004) 224–232
SURFACE & COATINGS TECHNOLOGY
www.elsevier.com/locate/surfcoat

Al–O–N based duplex coating system for improved oxidation resistance of superalloys and NiCrAlY coatings

S.K. Jha[a,b], Y.H. Sohn[a,*], S. Sastri[b], N. Gunda[b], J.A. Haynes[c]

[a]*Advanced Materials Processing and Analysis Center (AMPAC), University of Central Florida, Orlando, FL 32826, USA*
[b]*Surmet Corporation, Burlington, MA 01803, USA*
[c]*Oakridge National Laboratory, Oak Ridge, TN 3783, USA*

Received 7 April 2002; accepted in revised form 6 September 2003

Abstract

Performance of an Al–O–N based duplex coating system (DCS) was examined in order to improve the high-temperature oxidation resistance of superalloys and the low-pressure plasma sprayed NiCrAlY coatings. The DCS (~5 μm thick) was deposited using pulsed DC reactive magnetron sputtering as an external coating on Rene'N5 superalloy with and without NiCrAlY coating. DCS coatings were characterized using photo-stimulated luminescence spectroscopy, optical microscopy, scanning electron microscopy and energy-dispersive X-ray spectroscopy before and after high-temperature oxidation. As-deposited DCS contained varying amounts of α-, γ-Al_2O_3 and amorphous phases depending on the chemistry and surface characteristics of the substrate. Heat treatment at 1121 °C (2050 °F) for 2 h in air facilitated complete phase transformation to equilibrium α-Al_2O_3 in the DCS. Improvement in oxidation resistance was observed for DCS specimens during 250-h oxidation at 1121 °C (2050 °F). In particular, DCS was found to be very effective as an external coating on the rough (as-sprayed) NiCrAlY surface. The superior oxidation resistance of the specimens with DCS may be attributed to the formation of slow-growing and adherent alumina scale and the prevention of Ni/Cr-rich oxide formation.

Keywords: Oxidation; Thermally grown oxide; Coatings; Residual stress; Photostimulate luminescence

1. Introduction

The adherence and durability of thermally grown oxide (TGO) are critical to the long-term performance of high-temperature materials. Many high-temperature alloys and their coatings are designed to form a protective TGO scale against oxidizing environments. The factors that control oxidation-limited life of alloys and coatings are the growth kinetics of TGO scale, spallation of TGO scale during thermal cycling, change in composition of alloys and coatings due to TGO formation and interdiffusion. Integrity of the TGO scale is governed by the magnitude of elastic energy in the scale, which in turn is determined by the magnitude of residual stress (growth and thermal stresses) and the thickness of the scale. The scale thickness is determined by the diffusion of oxygen and/or metal ion through the scale (presumably through grain boundary diffusion) [1,2], and is generally represented by the parabolic rate constant, K_p [1]. The growth rate of an oxide scale strongly depends on oxidation temperature and composition of alloy and/or coating. For systems requiring extremely long lifetimes, even a moderate change in K_p can result in measurable changes in oxide thickness, metal consumption, elastic strain energy in the scale and consequently the lifetimes.

The loss of adhesion between the TGO/metal interface and the subsequent TGO spallation is especially dangerous in the case of thermal barrier coatings (TBCs), which are extensively employed to provide thermal protection of hot-section component in advanced turbine engines [3–7]. TBCs in general consist of a ceramic topcoat, a TGO scale, an intermediate bond coat (i.e. TGO former) and a superalloy substrate [3–7]. The failure of TBCs often occurs near the thermally grown aluminum oxide (TGAO) layer [3–13] due to compressive residual stress in the TGAO arising out of

*Corresponding author. Tel.: +1-407-882-1181; fax: +1-407-882-1462.
E-mail address: ysohn@mail.ucf.edu (Y.H. Sohn).

0257-8972/04/$ - see front matter © 2003 Elsevier B.V. All rights reserved.
doi:10.1016/j.surfcoat.2003.09.044

thermal expansion mismatch between the oxide and the underlying metal. Since TGAO forms between the ceramic top coat and the intermediate overlay bond coat, the failure of the TGAO scale will lead to permanent loss of the topcoat, and hence the loss of thermal insulation for metallic components. Failure of TGAO scale on a typical bond coat, MCrAlY (M = Ni and/or Co), is frequently associated with the compositional change in the TGO from alumina to a mixture of chromia and spinels due to the depletion of Al from the MCrAlY and concurrent enrichment of Ni, Cr and Co in the oxide [14–16]. The spinels begin to form instead of alumina when the Al activity in the bond coat decreases below 10^{-17} [17].

Development of MCrAlY coatings with improved oxidation resistance at elevated temperatures is thus a major challenge. One approach to overcome this challenge is to develop an additional coating or coating system, either as an external layer over the MCrAlY coating or as a diffusion barrier between superalloy substrate and the MCrAlY. In recent years, coating compositions, viz. TiN and TiC [18] or the Al–O–N system [19], have been considered for this purpose. The combination of the favorable physical and thermo-mechanical properties of coatings based on Al–O–N system [20–23] makes it a potential candidate for this application. A coating system based on Al–O–N is expected to enhance the oxidation resistance of the superalloy-MCrAlY system by reducing the TGAO growth rate, suppressing the formation of Ni/Cr/Co-rich oxides, and inhibiting the interdiffusion between the superalloy and MCrAlY coating.

The objective of the present investigation was to examine the suitability of an external duplex coating system (DCS) based on Al–O–N system to improve the high-temperature oxidation resistance of superalloy and NiCrAlY coating. An attempt was made to evaluate the compatibility and performance of such a coating system on Rene'N5 superalloy with and without NiCrAlY coatings. In this paper, characteristics of the DCS in terms of phase constituents, microstructure and residual stress are presented and discussed in the light of performance against high-temperature oxidation.

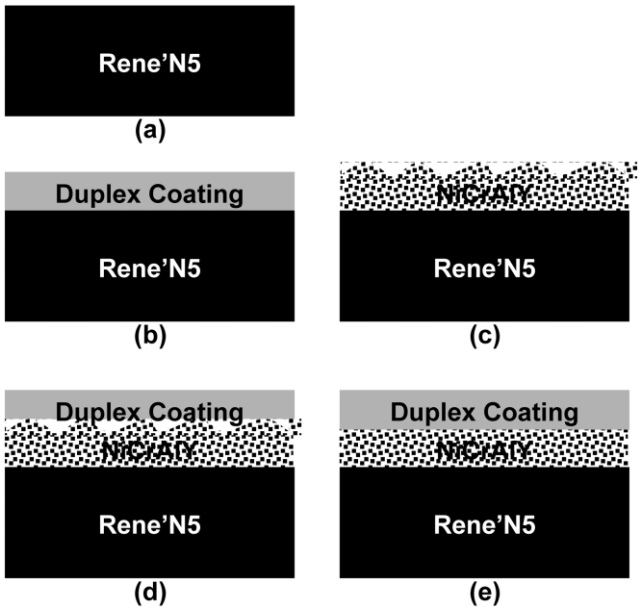

Fig. 1. Schematic illustration of specimens examined in this study: (a) stand-alone Rene'N5; (b) DCS coated Rene'N5; (c) NiCrAlY coated Rene'N5; (d) Rene'N5 coated with NiCrAlY (as-sprayed-rough surface) and DCS and (e) Rene'N5 coated with NiCrAlY (polished-smooth surface) and DCS.

2. Experimental details

Disk-shaped (16 mm diameter; 1.5 mm thick) single-crystal Rene'N5 superalloy specimens were coated with NiCrAlY and DCS in collaboration with Surmet Corporation, Burlington, MA. The nominal composition of the Rene'N5 is Ni–7.3Co–7.0Cr–6.4Ta–6.0Al–5.1W–3.0Re–1.4Mo–0.1Hf–0.01Ti–0.05C by wt.%. The DCS (~5 μm thick) and NiCrAlY (Ni–17%Cr–6%Al–0.5%Y wt.%) coating (~100 μm thick) were deposited, respectively, by the pulsed DC reactive magnetron sputtering and low-pressure plasma spraying. Specimens were prepared according to the specifications listed in Table 1. They are schematically illustrated in Fig. 1. Surface preparation was carried out by grinding (600 grit SiC) and polishing (alumina suspension, 1.0-μm final finish) to obtain Rene'N5 and NiCrAlY coatings with smooth surface. The polished surface was cleaned

Table 1
Specimen description for Rene'N5 superalloy disks coated with combination of NiCrAlY coatings and DCS

Superalloy substrate	VPS NiCrAlY	Surface finish of substrate[a] before the deposition of DSC	Duplex coating system
Single-crystal Rene'N5	None	Polished, smooth	None
	None	Polished, smooth	~5 μm
	~100 μm	As-sprayed, rough	None
	~100 μm	As-sprayed, rough	~5 μm
	~100 μm	Polished, smooth	~5 μm

[a] Refers to the surface finish of either Rene'N5 or NiCrAlY onto which DCS was deposited.

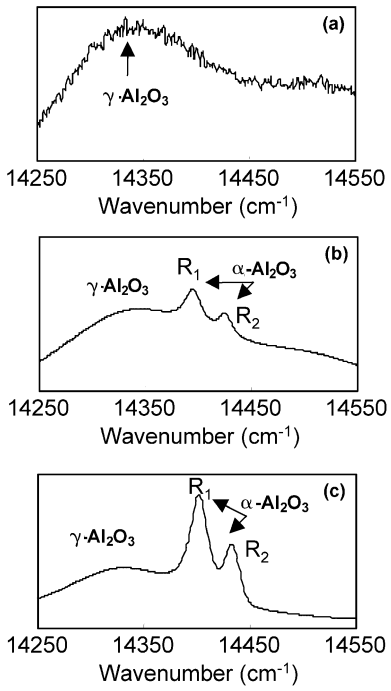

Fig. 2. Typical photostimulated luminescence spectra from the as-coated DCS on (a) Rene'N5; (b) polished-smooth NiCrAlY coatings and (c) as-sprayed-rough NiCrAlY coatings.

in water, ultrasonically degreased with acetone and dried prior to the deposition of DCS. The difference in surface preparation prior to DCS deposition emulate the rough and smooth bond coat surface for TBCs deposited by air plasma spray (APS) and electron beam physical vapor deposition (EB-PVD), respectively. The as-processed DCS specimens were subjected to heat-treatment at 1121 °C (2050 °F) for 2 h in air, in order to investigate the kinetics of the phase transformations in the DCS, and to assess the initial thermo-mechanical compatibility of DCS with substrates. This temperature was chosen with respect to the applications where Ni-base superalloys are employed for structural applications and the oxidation resistance plays a critical role in component durability.

All specimens were subjected to oxidation at 1121 °C (2050 °F) for 250 h in ambient air using a muffle furnace (Thermolyne F46100 with Eurotherm 2408 Temperature Controller). Again, this temperature was chosen with respect to the high-temperature application of DCS. Specimens were cleaned with water, ultrasonically degreased in acetone, dried and accurately weighed before the oxidation. They were arranged separately in small alumina crucibles and placed inside the furnace preheated to 1121 °C (2050 °F). Each specimen was taken out of the furnace after 25 h of oxidation and cooled to room temperature. After recording the weight gain, which included the weight of the specimens and spalled DCS–TGO flakes, specimens were put back in the furnace. This procedure was repeated until the completion of 250 total-hours of oxidation at 1121 °C (2050 °F).

To examine the surface morphology, microstructure and residual stress of the coatings and/or the oxide scale, optical microscopy, scanning electron microscopy, energy-dispersive spectroscopy (EDS) and photo-stimulated luminescence spectroscopy (PSLS) were employed. The residual stress in the DCS and/or oxide scale was measured on the basis of the piezospectroscopic shift in the photo-stimulated Cr^{3+} luminescence from trace Cr^{3+} impurity incorporated in the α-Al_2O_3; details of PSLS can be found in Refs. [24–27].

3. Results and discussion

3.1. As-deposited duplex coating system

Photo-luminescence from the amorphous and metastable γ-Al_2O_3 phases was observed as presented in Fig. 2a along with trace luminescence of α-Al_2O_3 from as-deposited DCS on Rene'N5. As-deposited DCS on NiCrAlY coating on Rene'N5 was found to consist of α- and γ-Al_2O_3 phases as seen from the photo-luminescence spectra in Fig. 2b and c. Relative intensities of the photo-luminescence from α-and γ-Al_2O_3, however, were different in the case of DCS on polished-smooth and as-sprayed-rough NiCrAlY. More γ-Al_2O_3 luminescence was observed from DCS coated on the polished-smooth NiCrAlY than DCS coated on as-sprayed-rough NiCrAlY. The relative intensity ratio in terms of fraction (i.e. the ratio of R_1–R_2 luminescence from α-Al_2O_3 to the total luminescence) as a function of the substrate type is presented in Fig. 3. It should be mentioned that Fig. 3 does not represent the actual volume fraction of α-Al_2O_3 in the DCS. Difference in surface finish may

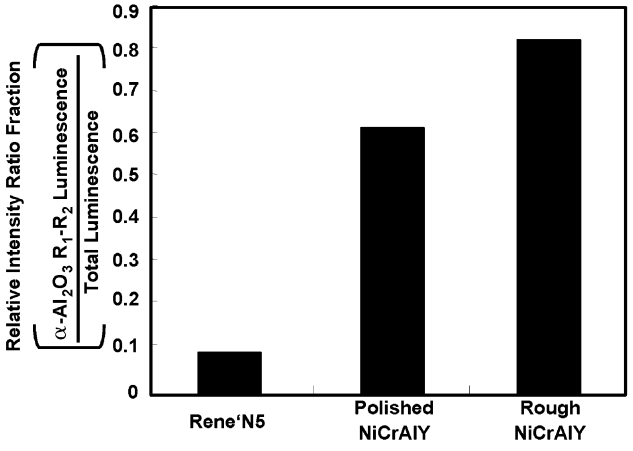

Fig. 3. Relative intensity ratio of photostimulated luminescence from α-Al_2O_3 in the as-coated DCS on different substrates. This fraction does not correspond to the actual volume fraction of α-Al_2O_3 phase in as-coated DCS.

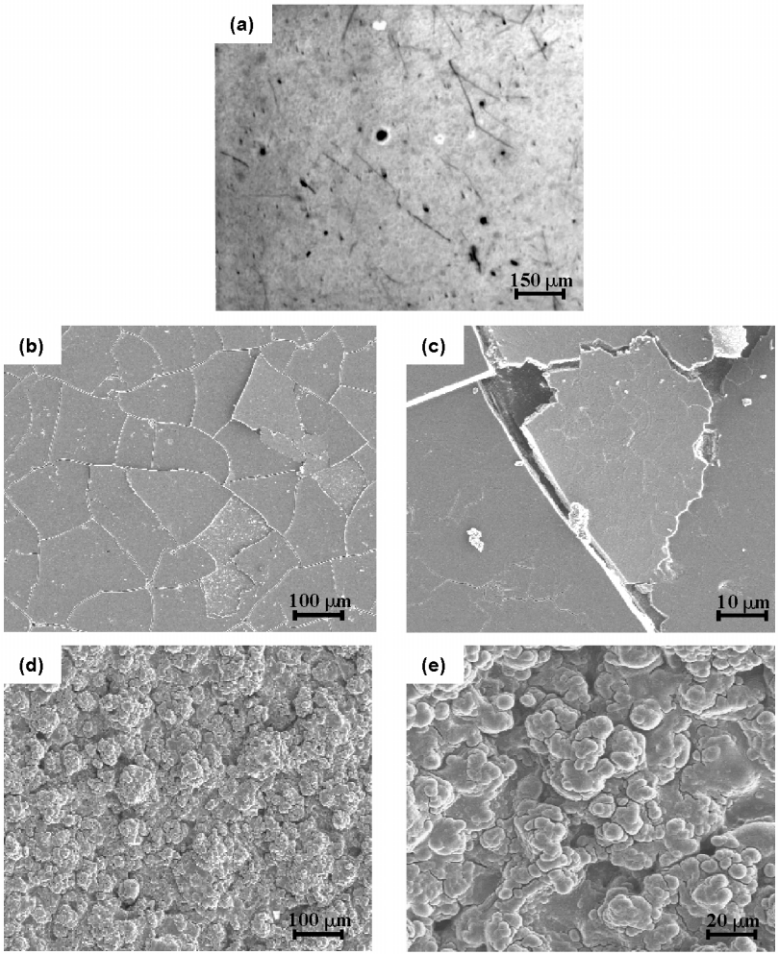

Fig. 4. Optical and secondary electron micrographs exhibiting morphology of heat-treated (1121 °C (2050 °F) for 2 h) DCS on (a) Rene'N5; (b and c) on polished-smooth NiCrAlY and (d and e) on as-sprayed-rough NiCrAlY.

be responsible for the apparent difference in DCS constituents. Rough surface of as-sprayed NiCrAlY surface may promote easier transition to equilibrium α-Al_2O_3 phase [28].

3.2. Heat-treated duplex coating system

Morphology of heat-treated DCS on Rene'N5, polished-smooth NiCrAlY and as-sprayed-rough NiCrAlY are presented in Fig. 4. Optical micrograph for Rene'N5-DCS in Fig. 4a shows some scratches on Rene'N5, due to the optically translucent nature of the DCS. DCS on polished NiCrAlY coating had many cracks and spallation as seen in Fig. 4b and c. On the other hand, the surface morphology of the heat-treated DCS on as-sprayed-rough NiCrAlY is relatively uniform and without cracks as seen in Fig. 4d and e, except for those from spat-quenched NiCrAlY coating underneath.

PSLS measurements were carried out on all specimens after heat-treatment. Luminescence only from α-Al_2O_3 (R_1 and R_2) phase was observed in all cases: typical luminescence only from α-Al_2O_3 (R_1 and R_2) phase is presented in Fig. 5. Equilibrium α-Al_2O_3 would be the desirable constituent in DCS to minimize the TGAO growth rate. Diffusion of metallic ions in γ-Al_2O_3 is much faster than α-Al_2O_3, due to partially occupied Al lattice sites ($\sim$21 of the 24 sites) in γ-Al_2O_3 [29]. For example, Becker et al. [30] found that, even at low oxygen partial pressure, γ-Al_2O_3 was able to dissolve 6–8 at.% Ti at 900 °C. Complete phase transformation to equilibrium α-Al_2O_3 in DCS would minimize the rate of TGAO growth, governed by the inward diffusion of oxygen through the TGAO [17,31,32].

PSLS data from 10 randomly selected locations were used for the measurement of residual stress in DCS, containing α-Al_2O_3 phase. Magnitude of compressive residual stress, determined on the basis of piezospectroscopic shift [24,25] of the photo-luminescence, indicated that α-Al_2O_3 is least compressively stressed for the as-sprayed-rough NiCrAlY ($\sigma_{comp} = 0.6 \pm 0.3$ GPa). Magnitude of compressive residual stress in α-Al_2O_3 was higher for the polished-smooth NiCrAlY ($\sigma_{comp} =$

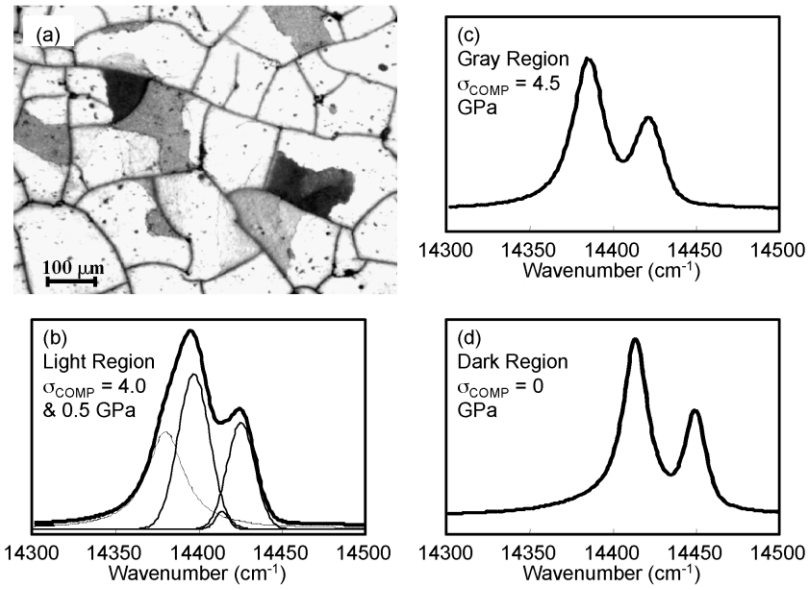

Fig. 5. Microstructure and residual stress of heat-treated (1121 °C (2050 °F) for 2 h) DCS on polished-smooth NiCrAlY surface. (a) Optical photomicrograph shows three distinctive regions. (b) Bimodal luminescence was observed from the light region. (c) The gray regions were highly compressively stressed and (d) the dark regions were stress-free.

1.7 ± 1.7 GPa) and for Rene'N5 ($\sigma_{comp} = 1.8 \pm 0.3$ GPa) substrates. The large standard deviation on polished-smooth NiCrAlY can be attributed to the stress-relief associated with the localized damage of coating shown in Fig. 4b and c.

Relationship between microstructural features and residual stress variation for the heat-treated DCS on polished-smooth NiCrAlY surface is illustrated in Fig. 5. Optical photomicrograph in Fig. 5 shows three distinctive contrast (light, gray and dark) regions on the top of the DCS coating. Typical photoluminescence spectra presented in Fig. 5b–d show that the magnitude of compressive residual stress varied significantly for these regions. Bimodal photo-luminescence (Fig. 5b) ($\sigma_{comp} \approx 4.0$ and 0.5 GPa) consisting of two sets of R_1–R_2 luminescence was obtained from the light region. One set of R_1–R_2 luminescence is believed to originate from the stressed component ($\sigma_{comp} \approx 4.0$ GPa), while the other is due to nearly stress-free component ($\sigma_{comp} \approx 0.5$ GPa) of the DCS and/or α-Al_2O_3 scale [33,34]. This observation could be due to partial stress-relief associated with the damage and/or phase transformation in the DCS. Gray regions in Fig. 5a represents oxidized (α-Al_2O_3) NiCrAlY surface with high magnitude of compressive residual stress ($\sigma_{comp} = \sim 4.5$ GPa) resulting from the heat-treatment and subsequent cooling to room temperature. In gray regions, DCS has spalled during heating period of the heat treatment and the exposed NiCrAlY surface was oxidized during the heat treatment. Dark region in Fig. 5a represents damaged

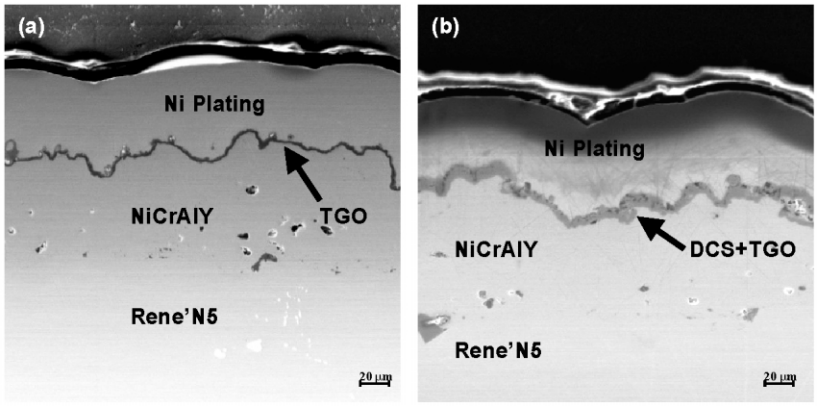

Fig. 6. Cross-sectional secondary electron micrographs of heat-treated (1121 °C (2050 °F) for 2 h) specimens: (a) NiCrAlY coated Rene'N5 and (b) DCS coated NiCrAlY (as-sprayed-rough) coatings on Rene'N5.

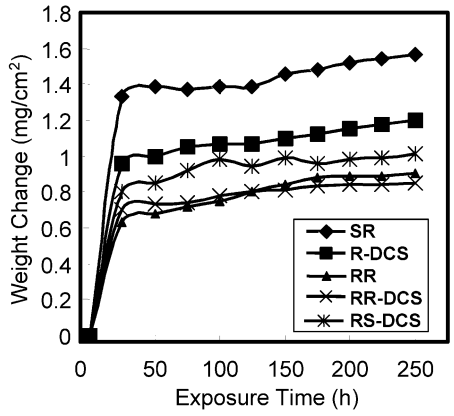

Fig. 7. Weight change vs. exposure time of various specimens oxidized at 1121 °C (2050 °F) in air. Spalled flakes of the TGO scale and/or DCS were included in the weight measurement. Legends SR, R-DCS, RR, RR-DCS and RS-DCS refer to stand-alone Rene'N5, Rene'N5 with DCS, NiCrAlY coated Rene'N5, DCS on as-coated-rough NiCrAlY with Rene'N5 substrate and DCS on polished-smooth NiCrAlY with Rene'N5 substrate, respectively.

DCS, corresponding to that shown in Fig. 4c with complete stress-relief. Presence of both gray (damaged and reoxidized) and dark (damaged) regions indicates that the DCS spallation from polished-smooth NiCrAlY surface occurred during both heating and cooling period of the heat treatment.

Cross-sections of heat-treated specimens, NiCrAlY coated Rene'N5 and DCS coated on as-sprayed-rough NiCrAlY coating on Rene'N5 are presented in Fig. 6. Typical microstructure of a thin (~2–3 μm) and continuous TGO layer on NiCrAlY coating is presented in Fig. 6a. A duplex layer (~7–8 μm) consisting of both TGO and DCS can be seen from Fig. 6b for the specimen coated with DCS on as-sprayed-rough NiCrAlY coating on Rene'N5. The TGO and/or DCS were uniform and continuous for both specimens.

3.3. Oxidation behavior of the duplex coating system

High-temperature oxidation test was carried out at 1121 °C (2050 °F) in air for 250 h for all specimens. Stand-alone Rene'N5 and Rene'N5 coated with NiCrAlY were also tested for comparison. The oxidation data plotted as specific weight change (mg/cm^2) vs. exposure time for all specimens are presented in Fig. 7. Measurements of specimen weight included weight gain due to oxidation and the spalled flakes of TGO and/or DCS. Lowest weight gain was observed for specimen coated with DCS on as-sprayed-rough NiCrAlY coated Rene'N5. Stand-alone Rene'N5 had the maximum weight gain.

3.4. Characterization of oxide scale

Visual inspection of the specimens during weight change measurements every 25 h of oxidation provided evidence of progressive TGO and/or DCS spallation in the case of stand-alone Rene'N5, DCS on smooth Rene'N5 and DCS on smooth NiCrAlY coatings. However, there was no evidence of TGO and/or DCS spallation for the specimen coated with NiCrAlY on Rene'N5 and the specimen coated with DCS on as-sprayed-rough NiCrAlY coating on Rene'N5.

3.4.1. DCS on polished-smooth NiCrAlY after oxidation

Surface morphology of the DCS on polished-smooth NiCrAlY after oxidation is shown in Fig. 8. Oxidized surface consisted of regions where oxide scale and/or DCS have spalled off during cooling, exposing the metallic NiCrAlY surface with TGO imprints as seen in Fig. 8b. This was also confirmed by EDS analysis where

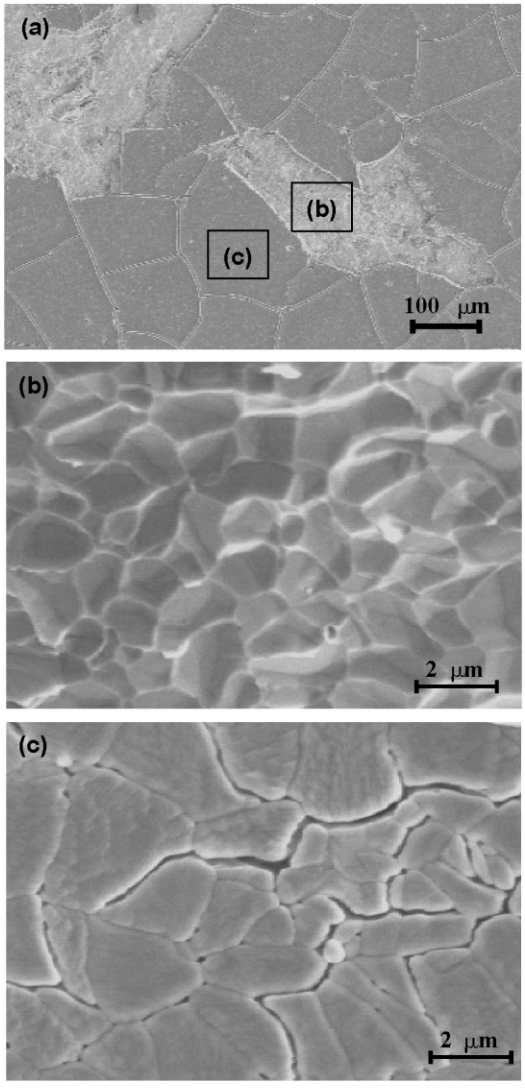

Fig. 8. Secondary electron micrographs showing the (a) surface morphology of DCS coating on polished-smooth NiCrAlY coated Rene'N5 after 250 h of oxidation at 1121 °C (2050 °F) in air: (b) exposed metallic surface with TGO imprints due to TGO spallation and (b) intergranular cracks in intact DCS.

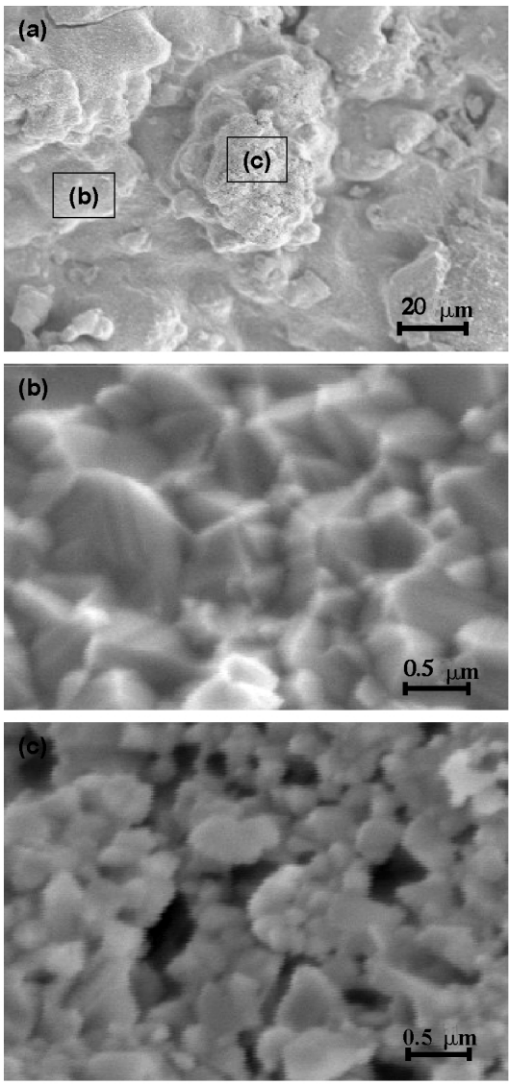

Fig. 9. Secondary electron micrographs showing (a) typical surface morphology of TGO on NiCrAlY coatings after 250 h of oxidation at 1121 °C (2050 °F) in air. Representative micrograph shows (b) surface morphology of dense, continuous α-Al_2O_3 and (c) porous oxide scale.

intensities of Ni, Cr and Al X-radiation correspond well with those of NiCrAlY coatings. This imprint morphology is associated with brittle fracture of the TGO/metal interface, and has been reported by several authors [35–37]. Intergranular cracks on surfaces were observed in region where DCS was intact as presented in Fig. 8c. Formation of these cracks and spallation of oxide and/or DCS would adversely affect the high-temperature oxidation resistance of these specimens.

3.4.2. Rene'N5-NiCrAlY and Rene'N5-NiCrAlY (as-sprayed, rough)-DCS after oxidation

A typical surface morphology of as-sprayed-rough NiCrAlY coatings on Rene'N5 (without DCS) after oxidation is shown in Fig. 9. Two morphologically distinctive regions representing continuous dense α-Al_2O_3 scale, Fig. 9b, and porous oxide scale, Fig. 9c, were observed. Surface morphology of the DCS coating on as-sprayed-rough NiCrAlY coated Rene'N5 is presented in Fig. 10. A typical morphology of continuous dense α-Al_2O_3 scale was uniformly observed as shown in Fig. 10b.

Cross-sectional secondary electron micrographs of the oxidized specimens of these two specimens are presented in Fig. 11. Oxide scale developed on NiCrAlY coatings consists of two distinct layers (light and dark) as presented in Fig. 11a. EDS shown in Fig. 11c suggests that the light region (top-layer) of the oxide scale contains oxides phases such as Cr_2O_3 and $Ni(Cr,Al)_2O_4$ spinels. The dark region consisted only of Al_2O_3 as seen in Fig. 11d. On the other hand, a uniform oxide scale consisting only of Al_2O_3 was found for the specimen with DCS on the as-sprayed-rough NiCrAlY as seen in Fig. 11b and e.

Formation of non-protective oxides in TGO, such as $Ni(Cr,Al)_2O_4$ spinels, can be detrimental to the oxidation resistance of a metal/coating system [38]. These usually increase in extent with the exposure time in oxidizing conditions at elevated temperatures, and thus limit the useful lifetime of the system. Results in this study suggest that the application of DCS as external coating

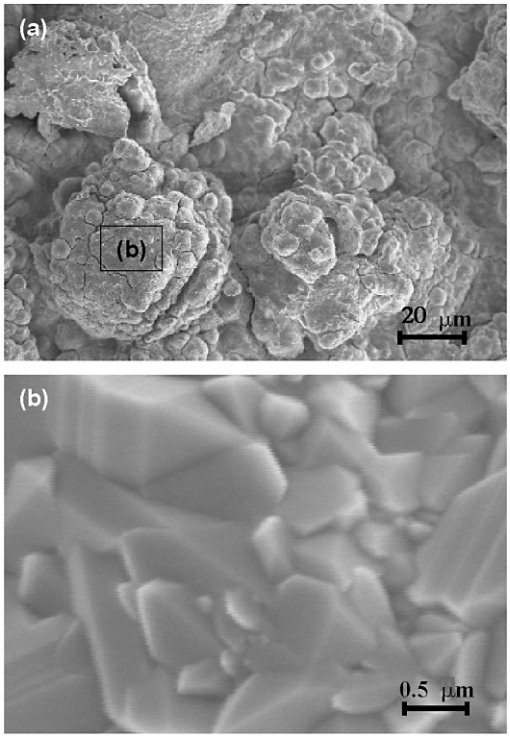

Fig. 10. Secondary electron micrographs showing (a) typical surface morphology of DCS coated on as-sprayed-rough NiCrAlY coating after 250 h of oxidation at 1121 °C (2050 °F) in air. (b) High magnification micrograph shows a region where surface morphology of α-Al_2O_3 is dense and continuous.

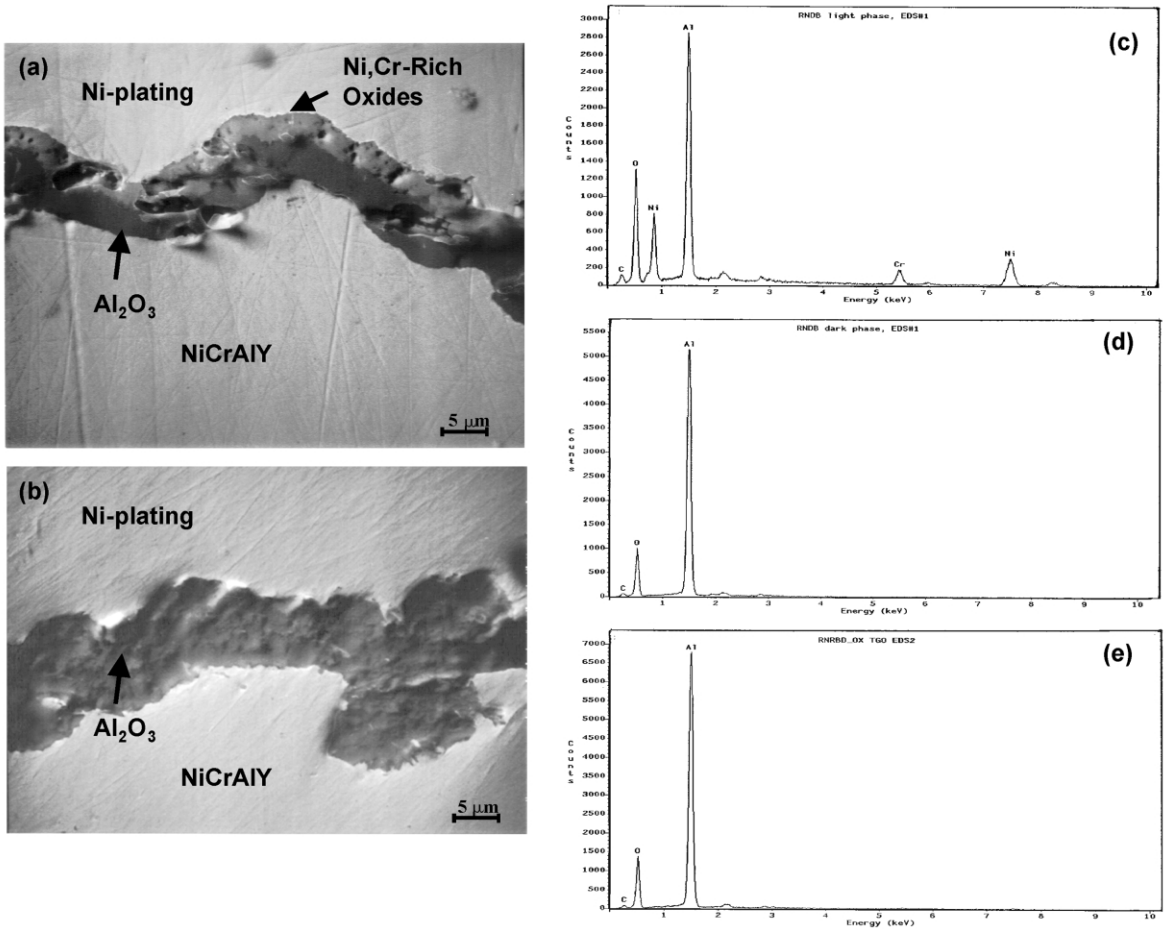

Fig. 11. Cross-sectional secondary electron micrographs of TGO scale, developed after 250 h of oxidation at 1121 °C (2050 °F) in air, on as-sprayed-rough NiCrAlY coating (a) without and (b) with DCS coating. TGO scale developed on NiCrAlY coating without DCS consists of two layers containing (c) Ni/Cr/Al-rich oxides and (d) Al-rich oxide. With the application of DCS coating, a single layer scale containing Al-rich oxide was observed to develop.

has helped to prevent the formation of non-protective oxides by promoting an anion-controlled (i.e. inward diffusion of oxygen through the alumina scale) oxidation to form a slow-growing α-Al_2O_3 [15,29,30]. On the other hand, without DCS, outward diffusion of Ni and Cr [39] has significantly contributed in the overall process of oxide scale formation.

3.4.3. Compressive residual stress of the DCS and/or TGO after oxidation

Compressive residual stress in DCS and/or oxide scale after 250 h of oxidation at 1121 °C (2050 °F) were determined on the basis of the PSLS data from 10 randomly selected locations of each specimen. The average value of the compressive residual stress for various specimens is presented in Fig. 12. Stress-free luminescence associated with spallation was excluded in the calculation of the average values. Extensive spallation of the oxide scale was observed during oxidation for stand-alone Rene'N5 and DCS coated specimens with extremely high magnitude of compressive

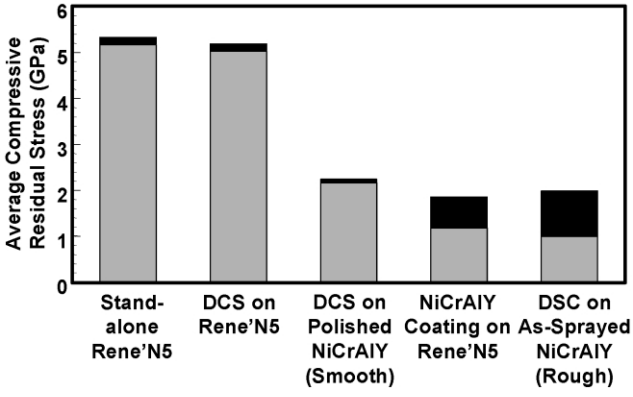

Fig. 12. Average values of the compressive residual stress in the α-Al_2O_3 scale and/or the DCS after 250 h of oxidation at 1121 °C (2050 °F) in air. Stress-free luminescence arising from TGO/DCS spallation was excluded from the calculation of average values.

residual stress of the α-Al_2O_3 scale. On the other hand, spallation of the oxide scale was not observed for the specimens Rene'N5-NiCrAlY and Rene'N5-NiCrAlY (rough)-DCS, whose compressive residual stresses were much lower. Thus, magnitude of compressive residual stress seems to play an important role in spallation of TGO scale, although the spallation resistance of a TGO scale cannot be determined solely on the basis of the magnitude of the residual stress in oxide scale.

4. Conclusions

Al–O–N based DCS was investigated to enhance high-temperature oxidation resistance of superalloy and NiCrAlY coating. The following conclusions were drawn from this investigation:

- As-deposited DCS contained varying amounts of amorphous, metastable γ-Al_2O_3 and equilibrium α-Al_2O_3 phases as a function of surface characteristic of the substrate.
- Heat-treatment facilitated the transformation of amorphous and metastable γ-Al_2O_3 to equilibrium α-Al_2O_3 phase in the DCS.
- Improvement in oxidation resistance was achieved by the application of DCS on as-sprayed (rough) NiCrAlY surface. The superior oxidation resistance of the system is attributed to its ability to form and maintain a slow-growing alumina scale during oxidation. DCS also helped to prevent the formation of Ni/Cr-rich oxides.

References

[1] P. Kofstad, High Temperature Corrosion, Elsevier, London/New York, 1988.
[2] R. Prescott, M.J. Graham, Oxid. Metals 38 (1992) 233.
[3] R.A. Miller, J. Thermal Spray Technol. 6 (1997) 35.
[4] R.A. Miller, Surf. Coat. Technol. 30 (1987) 1.
[5] T.E. Strangman, Thin Solid Films 127 (1985) 93.
[6] D.J. Wortman, B.A. Nagaraj, E.C. Duderstadt, Mater. Sci. Eng. A 121 (1989) 433.
[7] S.M. Meier, D.M. Nissley, K.D. Sheffler, S. Bose, J. Eng. Gas Turbine Power 114 (1992) 259.
[8] Y.H. Sohn, J.H. Kim, E.H. Jordan, M. Gell, Surf. Coat. Technol. 146–147 (2001) 70–78.
[9] E.Y. Lee, R.R. Biederman, R.D. Sisson Jr., Micro. Sci. 7 (1991) 505.
[10] M. Gell, K. Vaidyanathan, B. Barber, J. Cheng, E. Jordan, Met. Mater. Trans. A 30 (1999) 427.
[11] Y.H. Sohn, R.R. Biedermann, R.D. Sisson Jr., J. Mater. Eng. Perform. 3 (1994) 55.
[12] Y.S. Song, I.G. Lee, D.Y. Lee, D.J. Kim, S. Kim, K. Lee, Mater. Sci. Eng. A 332 (2002) 129.
[13] B. Wang, J. Gong, Y. Wang, C. Sun, R.F. Huang, L.S. Wen, Surf. Coat. Technol. 149 (2002) 70.
[14] D.P. Whittle, D.J. Evans, D.B. Scully, G.C. Wood, Acta Metall. 15 (1967) 1412.
[15] C.S. Giggins, F.S. Pettie, J. Electrochem. Soc. 118 (1971) 1782.
[16] J.A. Nesbitt, R.W. Heckel, Oxid. Metals 29 (1988) 75.
[17] M.J. Stiger, N.M. Yanar, M.G. Topping, F.S. Pettit, G.H. Meier, Z. Metallkd. 90 (1999) 1069.
[18] A.K. Telama, K.T. Torkell, T.A. Mantyla, P.O. Kettumen, in: W. Betz (Ed.), High Temperature Alloys for Gas Turbines and Other Applications, Part II, Redel, Dordrecht, 1986, p. 1081.
[19] O. Knotek, F. Loffler, W. Beele, Surf. Coat. Technol. 61 (1993) 6.
[20] C.F. Chen, E. Savrun, A.F. Ramirez, in: P. Vincenzini (Ed.), Ceramics Today—Tomorrows Ceramics, Elsevier, Amsterdam, 1991, p. 1295.
[21] W. Dehuang, G. Liang, Thin Solid Films 198 (1991) 207.
[22] R. Cremer, M. Witthaut, K. Reichert, M. Schierling, D. Neuschutz, Surf. Coat. Technol. 108–109 (1998) 48.
[23] S.D. Dvorak, O.D. Greenwood, W.N. William, R.J. Lad, Proc. Mater. Res. Soc. Symp. 522 (1998) 439.
[24] Q. Ma, D.R. Clarke, J. Am. Ceram. Soc. 76 (1993) 1433.
[25] J. He, D.R. Clarke, J. Am. Ceram. Soc. 78 (1995) 1347.
[26] Q. Wen, D.M. Lipkin, D.R. Clarke, J. Am. Ceram. Soc. 81 (1998) 3345.
[27] V.K. Tolpygo, D.R. Clarke, Mater. High Temp. 17 (2000) 59.
[28] J.A. Haynes, M.J. Lance, B.A. Pint, I.G. Wright, Elevated temperature coatings: science and technology IV, in: N.B. Dahotre, J.M. Hampikian, J.E. Morral (Eds.), The Minerals, Metals and Materials Society, 2001, p. 30.
[29] B. Schepers, H.D. Neuwinger, R. Stroka, in: E. Bartholome (Ed.), Ullmans Encyklopadie der technischen Chemie, 4. Auflage, Bd. 7, Verlag Chemie, Weinheim, 1974, p. 297.
[30] S. Becker, A. Rahmel, M. Schorr, M. Schutze, Oxid. Metals 38 (1992) 425.
[31] J.L. Smialek, B.K. Tubbs, Metall. Mater. Trans. A 26 (1995) 427.
[32] F.A. Golightly, F.H. Stott, G.C. Wood, Oxid. Metals 10 (1976) 163.
[33] J.A. Nychka, D.R. Clarke, Surf. Coat. Technol. 146–147 (2001) 110.
[34] Y.H. Sohn, K. Vaidyanathan, M. Ronski, E.H. Jordan, M. Gell, Surf. Coat. Technol. 146–147 (2001) 102.
[35] V.K. Tolpygo, D.R. Clarke, Acta Mater. 46 (1998) 5167.
[36] J.S. Wang, A.G. Evans, Acta Mater. 46 (1998) 4993.
[37] B.A. Pint, A.J. Garrat-Reed, L.W. Hobbs, Mater. High Temp. 13 (1995) 3.
[38] N.M. Yanar, G.H. Meier, F.S. Pettit, Scripta Mater. 46 (2002) 325.
[39] D.B. Dove, D.H. Baldwin, Metall. Trans. 5 (1974) 1637.